Analytical and Bioanalytical Chemistry
https://doi.org/10.1007/s00216-020-02493-z

RESEARCH PAPER

A microfluidic electrochemical flow cell capable of rapid on-chip dilution for fast-scan cyclic voltammetry electrode calibration

Lauren M. Delong[1] · Yuxin Li[1] · Gary N. Lim[1] · Salmika G. Wairegi[1] · Ashley E. Ross[1]

Received: 3 December 2019 / Revised: 13 January 2020 / Accepted: 5 February 2020

Abstract

Here, we developed a microfluidic electrochemical flow cell for fast-scan cyclic voltammetry which is capable of rapid on-chip dilution for efficient and cost-effective electrode calibration. Fast-scan cyclic voltammetry (FSCV) at carbon-fiber microelectrodes is a robust electroanalytical technique used to measure subsecond changes in neurotransmitter concentration over time. Traditional methods of electrode calibration for FSCV require several milliliters of a standard. Additionally, generating calibration curves can be time-consuming because separate solutions must be prepared for each concentration. Microfluidic electrochemical flow cells have been developed in the past; however, they often require incorporating the electrode in the device, making it difficult to remove for testing in biological tissues. Likewise, current microfluidic electrochemical flow cells are not capable of rapid on-chip dilution to eliminate the requirement of making multiple solutions. We designed a T-channel device, with microchannel dimensions of 100 μm × 50 μm, that delivered a standard to a 2-mm-diameter open electrode sampling well. A waste channel with the same dimensions was designed perpendicular to the well to flush and remove the standard. The dimensions of the T-microchannels and flow rates were chosen to facilitate complete mixing in the delivery channel prior to reaching the electrode. The degree of mixing was computationally modeled using COMSOL and was quantitatively assessed in the device using both colored dyes and electrochemical detection. On-chip electrode calibration for dopamine with FSCV was not significantly different than the traditional calibration method demonstrating its utility for FSCV calibration. Overall, this device improves the efficiency and ease of electrode calibration.

Keywords Electrochemistry · Microfluidics · T-channel · Carbon-fiber microelectrode · Flow cell · Dopamine

Introduction

Fast-scan cyclic voltammetry (FSCV) at carbon-fiber microelectrodes is an electroanalytical technique used to monitor subsecond neurochemical release and clearance in tissue [1, 2]. Over the last few decades, several advances in FSCV technology have been developed including new waveforms for selective analyte detection [3–6], novel electrode materials [7–12], and new hardware and software for improved background subtraction [13], basal level quantification [14], and electrode drift removal, among others [15]. Despite these advances, instrumentation for electrode calibration has remained primarily unchanged for the last several decades. Traditionally, electrode calibration is done using a six-port HPLC valve mounted on a two-position actuator controlled by a digital pneumatic solenoid. Milliliter volumes of standard solutions are required with this setup, providing an unnecessary cost disadvantage. Neurochemicals such as serotonin, purine nucleotides, and neuropeptides, which are often analyzed with FSCV [3, 16–21], can cost a few hundred dollars for just a few hundred milligrams. Additionally, constructing calibration curves requires several solutions, leading to a very time-consuming experiment and added cost. The traditional flow cell system for FSCV electrode calibration is also clunky and expensive, costing roughly two thousand US dollars. To overcome these disadvantages, we developed a microfluidic device capable of on-chip dilution of a standard solution for rapid and inexpensive electrode calibration curve generation for FSCV.

Published in the topical collection featuring *Female Role Models in Analytical Chemistry.*

Yuxin Li and Gary N. Lim contributed equally to this work.

✉ Ashley E. Ross
Ashley.ross@uc.edu

[1] University of Cincinnati – Chemistry, 312 College Dr., 404 Crosley Tower, Cincinnati, OH 45221-0172, USA

Published online: 17 February 2020

Microfluidics allows precise fluidic control of microliter volumes within micrometer-sized channels. Because of this, only small microliter volumes are needed. Microfluidic electrochemical flow cells for more traditional electroanalytical techniques, such as slow scan cyclic voltammetry and amperometry, have been developed prior for on-chip electrode calibration and detection [22–25]. Typically, these chips require embedding electrodes within the device; however, for FSCV, electrodes are removed from the flow cell after calibration and implanted in tissue, which prohibits the use of such devices for FSCV electrode calibration. Recently, Sinkala et al. developed an on-chip Y-channel flow cell calibration system for FSCV which yielded faster current rise times due to rapid switching between the standard and buffer; however, the dimensions of the fluidic channel were large requiring similar (mL) solution volumes used for traditional FSCV calibration [26]. Additionally, the device was not designed for rapid on-chip mixing which limits its ability to generate calibration curves quickly from a single standard concentration. For this reason, we have developed a new microfluidic flow cell for FSCV electrode calibration that allows an entire calibration curve to be generated from a single standard solution. The device design combined with the optimized flow rates allows for controlled dilution of a standard solution within seconds on-chip. Our microfluidic flow cell is an improvement over the traditional FSCV electrode calibration system because it costs significantly less, decreases the solution volume required to the microliters, and reduces the experimental time for generating calibrations curves.

Here, we have designed a T-channel microfluidic electrochemical flow cell which is capable of rapid on-chip dilution of a standard solution in order to construct full calibration curves from a single standard with FSCV. The length of the channel and flow rates were optimized to facilitate complete diffusion between the two fluid streams while also keeping the file collection window no greater than 60 s. Keeping the file collection window short is important for FSCV detection because it is a background-subtraction technique, where the background current is only stable for ~90 s. Electrode calibration is traditionally done by inducing a rapid concentration change at the electrode. The COMSOL Multiphysics software was used to simulate mixing on-chip and also estimate the time it takes the standard solution to reach the electrode in the electrode sampling well. Typical FSCV experiments require at least 10 mL of each standard concentration to generate a full calibration curve on a statistically relevant number of electrodes. With our device, we have decreased the required volume to 50 μL in total. In addition, a detailed comparison between the traditional flow cell and the microfluidic flow cell revealed no significant difference in calibration slopes and current detected, providing evidence that our chip is an acceptable platform for electrode calibration with FSCV. In the future, multiplexed detection platforms could be fabricated in order to further increase the throughput of electrode calibration.

Materials and methods

Chemical reagents

All reagents were purchased from Fisher Scientific unless otherwise noted. Stock dopamine solutions were stored in 0.1 M HCl at 4 °C. On the day of the experiment, dopamine was diluted to 15 μM in Tris buffer. Tris buffer contained 15 mM Tris(hydroxymethyl) aminomethane, 1.25 mM NaH_2PO_4, 2.0 mM Na_2SO_4, 3.25 mM KCl, 140 mM NaCl, 1.2 mM $CaCl_2$ dehydrate, and 1.2 mM $MgCl_2$ at pH 7.4. All aqueous solutions were made with Milli-Q water (Millipore, Billerica, MA).

Microfabrication of on-chip flow cell

The device was fabricated using standard soft lithography techniques [27, 28]. The device consisted of two layers: bottom layer (channels) and top layer (inlet holes). Transparency masks were created in AutoCAD 2020 and printed by CAD/Art Services Inc. (Bandon, OR) at 20,000 DPI. Master molds on 3″ silicon wafers (University Wafer, Boston, MA) were fabricated using SU-8 3050 (Microchem, Westborough, MA) photolithography in a class 1000 clean room. To create replicas, polydimethylsiloxane (PDMS, Ellsworth Adhesives, Germantown, WI) was mixed in a 10:1 ratio of silicon elastomer base to curing agent, poured over the device, degassed, and allowed to cure in the over for several hours at 65 °C. Once cured, the layers were removed from the silicon wafers using a scalpel. The electrode sampling well was punched out of the top layer using a 2-mm tissue punch (World Precision Instruments). The outlet and inlets for tubing were punched out of the top layer with a 0.75-mm tissue punch (Robbins Instruments, Chatham, NJ). The inlet/outlet holes were compatible with nonshrinkable PTFE TT-30 tubing with a 0.012″ I.D. and 0.009″ wall thickness (Weico Wire, Edgewood, NY). The bottom and top layer was manually aligned and bonded using air plasma treatment (SPI Plasma Prep III, SPI Supplies, West Chester, PA).

On-chip dilution of colored dyes

Colored dyes were used to visualize dilution on-chip. A red dye (20 μL of dye in 1 mL of water) was delivered down one inlet, and a blue dye (20 μL of dye in 1 mL of water) was delivered down the other inlet of the T-channel. Delivery was achieved using a Fusion 100 syringe pump (Chemyx,

Stafford, TX) and 50-μL Hamilton Model 1710 RN syringes with a 27-s gauge, large hub needle. Table 1 shows the flow rate combinations used to dilute the red dye in the channel (total flow rate in channel did not exceed 1 μL/min). Delivery continued until the electrode well was half filled. Images of the well were taken using a cell phone connected to a stereomicroscope (Fisher Scientific) set to 1.2×. The dye was removed at a rate of 2 μL/min from the well using a Fusion 200 Chemyx pump (pull mode) and a syringe connected to the waste outlet. The red mean value was averaged across the entire well of an unadjusted image using ImageJ.

Electrode fabrication

Fabrication of the cylindrical carbon-fiber microelectrodes followed the same procedure as previously described [18]. Briefly, a 7-μm T-650 carbon-fiber (Gift from Mitsubishi Chemical Carbon Fiber and Composites Inc., Sacramento, CA, USA) was aspirated into a glass capillary tube (A&M Systems, Sequim, WA, USA). A vertical Narishige PE-22 Electrode Puller (Tokyo, Japan) was used to pull the glass capillary into two microelectrodes. A scalpel (TedPella, CA, USA) was used to cut the excess carbon-fiber to 50–100 μm under a microscope (Fisher Education, USA). Prior to use, the microelectrodes were soaked in pure isopropyl alcohol for at least 10 min and back-filled with 1 M KCl solution to provide electrical connection.

Fast-scan cyclic voltammetry off-chip and on-chip

Fast-scan cyclic voltammograms were collected using a Pine Instruments WaveNeuro potentiostat (Durham, NC) with a 5-MΩ headstage. Data was collected using the HDCV analysis software (UNC Chapel Hill) and a PCIe-6363 computer interface board (National Instruments, Austin, TX). A triangular waveform scanning from − 0.4 to + 1.3 V and back was applied at 400 V/s with a repetition rate of 10 Hz. For off-chip FSCV calibrations, the traditional flow injection analysis system was used as previously reported with a flow rate of 1 mL/min using a Fusion 200 two-channel syringe pump (Chemyx, Stafford, TX) [29].

Table 1 Flow rate combinations to construct a calibration curve from a single inlet standard (15 μM) while maintaining the total flow rate in the channel at 1 μL/min

Inlet channel	Flow rate combinations (μL/min)				
Buffer	0.333	0.533	0.667	0.800	0.933
Standard	0.667	0.467	0.333	0.200	0.067
Concentration[a]	10 μM (1)	7 μM (2)	5 μM (3)	3 μM (4)	1 μM (5)

[a] In parenthesis are number codes associated with flow rate combinations

For on-chip calibration, the carbon-fiber microelectrode and Ag/AgCl reference electrode were placed in the electrode sampling well of the microfluidic flow cell and equilibrated for 10 min (see Fig. 1 for microelectrode placement). Each delivery of dopamine to the electrode was completed as follows: Three separate 50-μL Hamilton Model 1710 RN syringes with a 27-s gauge, large hub needle for dopamine and two for Tris buffer were connected to the two inlets of the T-channel and to the waste inlet (Fig. 1). The total flow rate was held constant at 1 μL/min in the delivery channel for the entire calibration time. For the first 10 s, Tris buffer was delivered down the channel at 1 μL/min and also delivered into the waste inlet at a rate of 1 μL/min. Buffer was removed from the waste outlet at a rate of 2 μL/min using a reverse pull Chemyx pump in order to avoid overflow in the electrode sampling well. After 10 s of background collection, dopamine was delivered down the inlet for standards, while keeping the buffer inlet on. The syringe for the standard solution contained 15 μM dopamine. The individual flow rates for dopamine and buffer were varied (while keeping the total flow rate constant, see Table 1) in order to control the concentration of dopamine delivery to the electrode. Effective mixing in the channel was validated using COMSOL Multiphysics simulations (see in "COMSOL Multiphysics modeling"). The dopamine-to-buffer solution was flowed for 20 s then turned off, and buffer alone was delivered at 1 μL/min for an additional 30 s. The solution was removed from the well using a Chemyx Fusion 200 pull pump. Buffer delivery down the T-channel inlet and in the waste inlet flushed out the channel and electrode well in between standard concentrations.

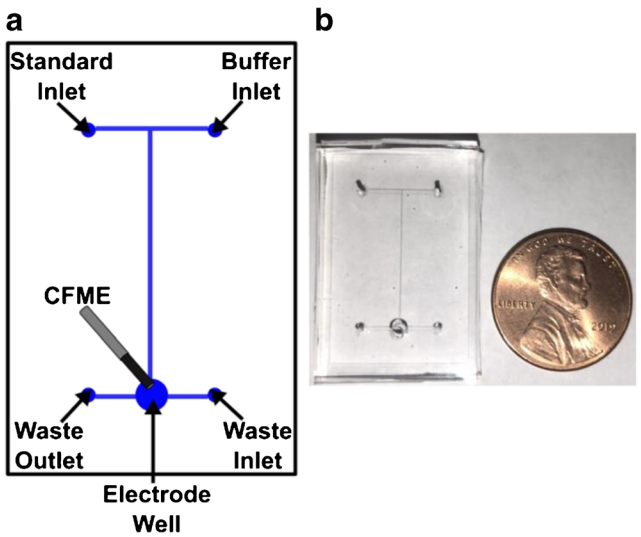

Fig. 1 Schematic and image of a microfluidic flow cell device designed to facilitate quick mixing on-chip for rapid electrochemical concentration curve generation from a single inlet concentration of a standard. **a** Top-view schematic of the device showing the buffer inlet, standard inlet (DA), electrode sampling well, and the waste inlet and outlet (reference electrode not shown). Cartoon carbon-fiber microelectrode (CFME) drawn to demonstrate placement in the well. **b** Image of the device, with a coin shown to demonstrate device size

COMSOL Multiphysics modeling

A computational model was used to predict the concentration of delivered dopamine to the electrode and compare it to the calculated delivery concentration based on the two inlet flow rates. The purpose of the model was to verify that complete mixing of the two fluid streams (from buffer and DA) occurs prior to delivery to the electrode. The three-dimensional model was built in COMSOL Multiphysics 5.4. The model incorporated the incompressible Navier-Stokes equation for fluid flow through the channel and transport of diluted species (using COMSOL modules laminar flow and transport of diluted species). Fluid flowed into 100 μm wide by 50 μm tall by 17 mm in length channel and out through the waste outlet set to atmospheric pressure. The buffer solution was modeled with the density and viscosity of water, 1000 kg/m^3 and 1.00 mPa s, respectively. The dopamine solution was modeled as 15 μM dopamine in an aqueous solution with a density and viscosity of water, 1000 kg/m^3 and 1.00 mPa s, respectively. The diffusion coefficient for dopamine (6×10^{-10} m^2/s) [30] in aqueous media was used to predict the degree of diffusion (using Fick's law) of dopamine across the channel (degree of mixing) prior to elution at the electrode sampling well. The buffer and dopamine inlet flow velocity was varied (see Table 1 for calculated inlet flow rates), while keeping the total flow rate through the channel constant at 1 μL/min. The concentration of dopamine in the electrode sampling well was determined in the center of the well and plotted as a function of the flow rate ratios (see Fig. 2).

Statistics

All statistics were performed in GraphPad Prism Version 8 (GraphPad Software Inc., La Jolla, CA). Statistical p values were considered significant at the 95% confidence level ($p < 0.05$). All values are reported as mean ± standard error of the mean (SEM). The n values represent either number of electrodes or number of devices.

Results and discussion

Device design for rapid and low-cost electrode calibration

A microfluidic device was designed to allow on-chip dilution of standards for rapid and low-cost electrode calibration curve generation for FSCV. The device is a two-layer microfluidic device which includes a T-channel, 100-μm (w) × 50-μm (h) × 17-mm (l) microchannels, that deliver to a 2 mm in diameter open electrode sampling well (Fig. 1). A 100-μm × 50-μm microchannel perpendicular to the electrode sampling well was used to flush the well and remove waste (Fig. 1). The

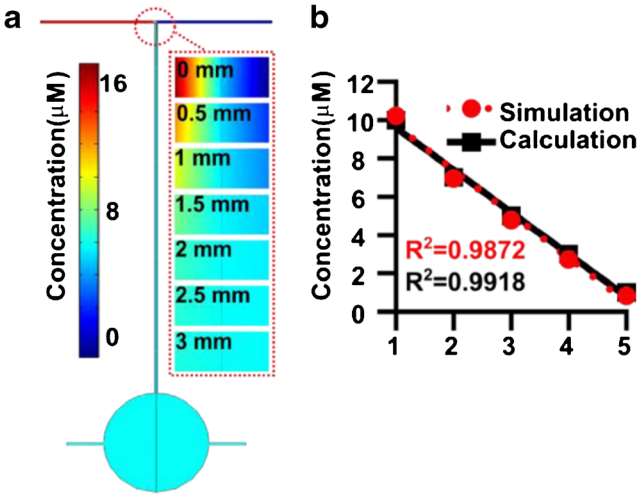

Fig. 2 Complete mixing occurs within the first 3 mm of the microfluidic channel. COMSOL Multiphysics simulations were used to model the degree of mixing within the channel and to estimate the concentration of DA in the electrode sampling well as a function of varying the inlet flow rates. The dopamine inlet (red) was simulated at a starting concentration of 15 μM. The total flow rate in the channel was held constant at 1 μL/min. **a** Inlet flow rate ratios of 1:1 (0.5 μL/min each) predict 7.5 μM DA (diluted by half) by 3 mm into the channel and in the electrode sampling well. **b** To verify that predictable dilution occurs across multiple flow rate ratios, the total flow rate in the channel was held constant at 1 μL/min, but the ratio of buffer to DA was varied to dilute DA in the well (see Table 1 for flow rate combinations). The simulated concentrations were plotted as a function of flow rate combination (numbered for simplicity) and compared with the expected concentration based on the dilution factor. Concentration decreased predictably in the well as the buffer flow rate increased and dopamine flow rate decreased. The simulated (red) and calculated (black) concentrations were approximately the same

T-channel inlets were used to deliver buffer in one inlet and dopamine solution in the other. The T-channel, combined with low flow rates (Table 1), was designed to facilitate efficient and complete mixing in the microchannel prior to reaching the electrode. This design allows the construction of a complete calibration curve, using only one standard solution. In addition, the T-channel design affords the ability to rapidly flush out the channel in between trials without needing to reload syringes.

On-chip mixing confirmed using COMSOL Multiphysics modeling

A computational model was used to provide evidence that mixing occurs in the microchannel prior to delivery to the electrode and the concentration is predictable. Figure 2a shows a COMSOL image demonstrating that complete mixing occurs within the first 3 mm of the delivery channel. In this example, the dopamine inlet (red) and buffer inlet (blue) were each delivered at a flow rate of 0.5 μL/min each (1:1 ratio). The starting dopamine concentration was 15 μM. By 3 mm down the delivery channel, the dopamine

concentration across the length of the channel equaled approximately 7.5 μM, indicating that it was diluted by half. This result is predictable based on the 1:1 flow rate ratio. To validate that a linear calibration curve could be constructed on this device and that the concentrations delivered to the electrode were predictable based on the dilution factor in the channel, we ran the model at varying inlet flow rates while keeping the total flow rate in the channel constant (Fig. 2b; see Table 1 for flow rate combinations). The starting concentration of dopamine in the channel was held constant at 15 μM. As expected, concentration decreased with increasing buffer flow rate (Fig. 2b, blue) and decreasing dopamine flow rate (Fig. 2b, red) and matched the calculated concentration value based on the dilution factor (Fig. 2b, black). The concentrations chosen for this analysis are within dopamine's linear range with FSCV at carbon-fiber microelectrodes [18].

On-chip mixing of colored dyes

A qualitative assessment using colored dyes demonstrated on-chip mixing (Fig. 3). Red and blue food coloring diluted in water was delivered down each inlet and a micrograph image was taken of the sampling well at each flow rate ratio (Fig. 3a, b for experiment schematic and Fig. 3c, d for images; see Table 1 for flow rates). The red value in each micrograph image was calculated using ImageJ and plotted as a function of flow rate ratio (Fig. 3d). Similar to the computational model, the red value changed as a function of increasing the blue dye inlet flow rate with decreasing the red dye inlet flow rate and was linear (Fig. 3e). This experiment demonstrated visually the dilution that occurs within the microchannel prior to delivery in the open sampling well.

Electrochemical dopamine detection on-chip

Electrochemical electrode calibration of dopamine on-chip was statistically similar to the traditional flow injection analysis system for FSCV providing evidence that the chip is an effective tool for electrode calibration. Five electrodes were pre-calibrated with 5 μM dopamine on the traditional flow injection analysis system. These same five electrodes were tested on-chip at the same concentration. An on-chip dilution from 15 μM dopamine to 5 μM dopamine was done by controlling the inlet flow rates: the inlet flow rate for buffer was 0.667 μL/min and the inlet flow rate for dopamine was 0.333 μL/min (flow rate combination #3, Table 1). An example color plot for both off-chip (Fig. 4a) and on-chip (Fig. 4b) and cyclic voltammograms (Fig. 4c) demonstrate similar currents for the same electrode. A longer file (60 s) was required for on-chip calibration due to the length of the delivery channel and the flow rates. On average, current was not significantly different between on-chip and off-chip for 5 μM dopamine

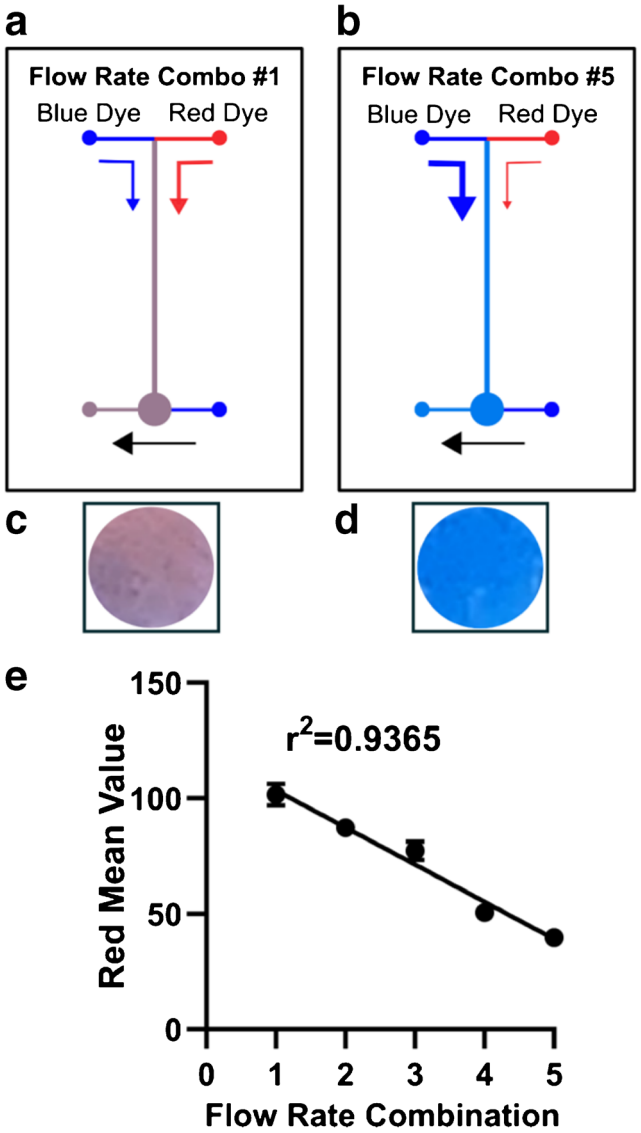

Fig. 3 Qualitative assessment of mixing using red and blue dye demonstrates predictable dilution on-chip. Top-view schematic of experiment at flow rate combination (see Table 1 for rates) #1 (**a**) and #5 (**b**). The thicker arrow indicates faster flow rate. The black arrow under the sampling well represents removal of standard from the well (**c**). Example micrograph images of the well at flow rate combination #1 and #5 (**d**). The red value in each micrograph was calculated using ImageJ and plotted as a function of flow rate combination #. On average, the red value decreases as a function of increasing the blue channel inlet flow rate with decreasing the red channel inlet flow rate, and is linear (**e**). This provides evidence that the degree of dilution is predictable ($n = 3$)

(paired t test, $p > 0.05$, $n = 5$). To verify reproducibility across devices, 5 μM dopamine was delivered, as before, to the same electrode on three separate devices. The average current detected was 77 ± 3 nA. The small value in the error demonstrates that on-chip dilution is reproducible across devices. This data demonstrates that the on-chip microfluidic flow cell is a reliable method for on-chip dilution and electrode calibration.

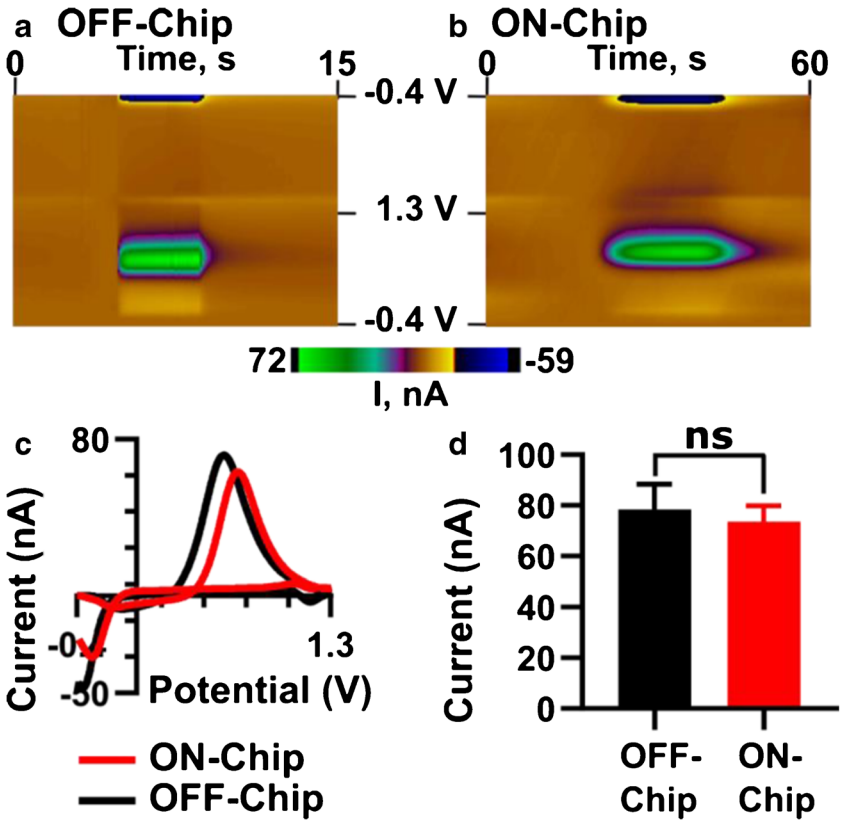

Fig. 4 The current detected for DA on-chip is not significantly different than the traditional flow cell. Example color plots for detection of 5 μM (prepared) DA off-chip (a) and 15 μM diluted to 5 μM DA on-chip (b). Example data for both off-chip and on-chip was collected on the same electrode so the currents could be compared. Color plot shows voltage on the *y*-axis and time on the *x*-axis, and current is shown in false color. The time file for on-chip detection is 60 s due to the time it takes dopamine to travel down the channel and reach the electrode. Example cyclic voltammograms for on-chip (red) and off-chip (black) on the same electrode (c). On average, current is not significantly different between on-chip and off-chip detection ($p > 0.05$, $n = 5$) for the same set of electrodes (d)

The calibration slopes on the same set of electrodes are not significantly different between on-chip and off-chip. A set of five electrodes were pre-calibrated using the traditional flow injection analysis system at concentrations within the range typically used to generate calibration curves for dopamine: 1, 3, 5, 7, and 10 μM dopamine (Fig. 5, black) [31–33]. This set of electrodes was subsequently calibrated on-chip at the same concentrations, using the flow rate combinations from Table 1 (Fig. 5, red). The slopes of the off-chip and on-chip regression line are 11.8 ± 1.5 nA/μM and 12.6 ± 1.0 nA/μM, respectively. The slopes for both methods were not significantly different ($p > 0.05$, $n = 5$) providing further evidence that the microfluidic flow cell is an acceptable platform for electrode calibration.

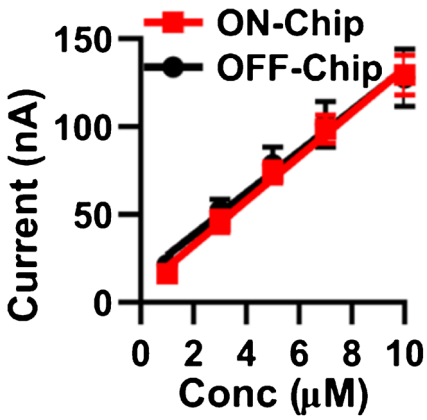

Fig. 5 The slopes of the calibration curves are statistically the same on-chip and off-chip ($p > 0.05$). The same set of electrodes ($n = 5$) were used both on-chip (red) and in the traditional flow cell (off-chip, black). The concentrations tested ranged from 1 to 10 μM

Conclusions

We developed a microfluidic electrochemical flow cell for carbon-fiber microelectrode calibration for FSCV. The data collected from the microfluidic flow cell is highly comparable with that from the traditional electrochemical flow cell for FSCV. Further, the microfluidic device is capable of rapid on-chip dilution by manipulating the inlet flow rates in the T-channel. This allows for the full linear range of many neurochemicals to be tested from a singly prepared standard solution. By reducing the need to make several solutions in combination with the dimensions of the device, a significant decrease in required solution

volume was achieved. The reduction in solution volume can significantly reduce the cost for particularly expensive neurochemicals. In addition, less preparation time is needed to calibrate electrodes. Overall, microfluidic electrochemical flow cells provide an efficient and low-cost alternative for electrode calibration for FSCV.

Acknowledgments We would like to thank Jeff Simkins in the CEAS Cleanroom at the University of Cincinnati for assistance in the facility.

Funding information Salmika Wairegi received funding from the NSF REU program for her 2019 summer research project.

Compliance with ethical standards

Conflict of interest The authors declare that they have no conflicts of interest.

References

1. Robinson DL, Venton BJ, Heien MLAV, Wightman RM. Detecting subsecond dopamine release with fast-scan cyclic voltammetry in vivo. Clin Chem. 2003;49:1763–73.
2. Roberts JG, Sombers LA. Fast-scan cyclic voltammetry: chemical sensing in the brain and beyond. Anal Chem. 2018;90:490–504. https://doi.org/10.1021/acs.analchem.7b04732.
3. Calhoun SE, Meunier CJ, Lee CA, McCarty GS, Sombers LA. Characterization of a multiple-scan-rate voltammetric waveform for real-time detection of met-enkephalin. ACS Chem Neurosci. 2019;10:2022–32. https://doi.org/10.1021/acschemneuro.8b00351.
4. Cryan MT, Ross AE. Scalene waveform for codetection of guanosine and adenosine using fast-scan cyclic voltammetry. Anal Chem. 2019;91:5987–93. https://doi.org/10.1021/acs.analchem.9b00450.
5. Jackson BP, Dietz SM, Wightman RM. Fast-scan cyclic voltammetry of 5-hydroxytryptamine. AnalChem. 1995;67:1115–20.
6. Cooper SE, Venton BJ. Fast-scan cyclic voltammetry for the detection of tyramine and octopamine. Anal Bioanal Chem. 2009;394:329–36. https://doi.org/10.1007/s00216-009-2616-0.
7. Yang C, Wang Y, Jacobs CB, Ivanov IN, Venton BJ. O2 plasma etching and antistatic gun surface modifications for CNT yarn microelectrode improve sensitivity and antifouling properties. Anal Chem. 2017;89:5605–11. https://doi.org/10.1021/acs.analchem.7b00785.
8. Cao Q, Hensley DK, Lavrik NV, Venton BJ. Carbon nanospikes have better electrochemical properties than carbon nanotubes due to greater surface roughness and defect sites. Carbon. 2019;155:250–7. https://doi.org/10.1016/j.carbon.2019.08.064.
9. Schmidt AC, Wang X, Zhu Y, Sombers LA. Carbon nanotube yarn electrodes for enhanced detection of neurotransmitter dynamics in live brain tissue. ACS Nano. 2013;7:7864–73. https://doi.org/10.1021/nn402857u.
10. Li Y, Ross AE. Plasma-treated carbon-fiber microelectrodes for improved purine detection with fast-scan cyclic voltammetry. Analyst. 2019. https://doi.org/10.1039/C9AN01636H.
11. Boateng A, Irague F, Brajter-Toth A. Low nM detection limits at porous 1–3 nm thick membrane-coated nanostructured microdisk electrodes. Electroanalysis. 2013;25:345–55. https://doi.org/10.1002/elan.201200489.
12. Kathiwala M, Affum A, Perry J, Brajter-Toth A. Direct measurements of xanthine in 2000-fold diluted xanthinuric urine with a nanoporous carbon fiber sensor. Analyst. 2008;133:810–6. https://doi.org/10.1039/b718125f.
13. Hermans A, Keithley RB, Kita JM, Sombers LA, Wightman RM. Dopamine detection with fast-scan cyclic voltammetry used with analog background subtraction. Anal Chem. 2008;80:4040–8. https://doi.org/10.1021/ac800108j.
14. Atcherley CW, Laude ND, Parent KL, Heien ML. Fast-scan controlled-adsorption voltammetry for the quantification of absolute concentrations and adsorption dynamics. Langmuir. 2013;29:14885–92. https://doi.org/10.1021/la402686s.
15. Meunier CJ, McCarty GS, Sombers LA. Drift subtraction for fast-scan cyclic voltammetry using double-waveform partial-least-squares regression. Anal Chem. 2019;91:7319–27. https://doi.org/10.1021/acs.analchem.9b01083.
16. Hashemi P, Dankoski EC, Lama R, Wood KM, Takmakov P, Wightman RM. Brain dopamine and serotonin differ in regulation and its consequences. PNAS. 2012;109:11510–5. https://doi.org/10.1073/pnas.1201547109.
17. Abdalla A, Atcherley CW, Pathirathna P, Samaranayake S, Qiang B, Peña E, et al. In vivo ambient serotonin measurements at carbon-Fiber microelectrodes. Anal Chem. 2017;89:9703–11. https://doi.org/10.1021/acs.analchem.7b01257.
18. Lim GN, Ross AE. Purine functional group type and placement modulate the interaction with carbon-fiber microelectrodes. ACS Sens. 2019;4:479–87. https://doi.org/10.1021/acssensors.8b01504.
19. Cryan MT, Ross AE. Subsecond detection of guanosine using fast-scan cyclic voltammetry. Analyst. 2018;144:249–57. https://doi.org/10.1039/C8AN01547C.
20. Xu YD, Venton BJ. Microelectrode sensing of adenosine/adenosine-5'-triphosphate with fast-scan cyclic voltammetry. Electroanalysis. 2010;22:1167–74. https://doi.org/10.1002/elan.200900559.
21. Schmidt AC, Dunaway LE, Roberts JG, McCarty GS, Sombers LA. Multiple scan rate voltammetry for selective quantification of real-time enkephalin dynamics. Anal Chem. 2014;86:7806–12. https://doi.org/10.1021/ac501725u.
22. Yuji M, Toshifumi T, Kenji Y, Eiichi T, Isao K, Masayuki S. Integration of enzyme-immobilized column with electrochemical flow cell using micromachining techniques for a glucose detection system. Anal Chem. 1993;65:2731–5. https://doi.org/10.1021/ac00068a005.
23. Murakami Y, Uchida T, Takeuchi T, Tamiya E, Karube I, Suda M. Micromachined electrochemical flow cell for biosensing. Electroanalysis. 1994;6:735–9. https://doi.org/10.1002/elan.1140060904.
24. del Campo FJ. Miniaturization of electrochemical flow devices: a mini-review. Electrochem Commun. 2014;45:91–4. https://doi.org/10.1016/j.elecom.2014.05.013.
25. Lin Y, Lu X, Gao X, Cheng H, Ohsaka T, Mao L. A new microfluidic chip-based online electrochemical platform for extracellular neurochemicals monitoring in rat brain. Electroanalysis. 2013;25:1010–6. https://doi.org/10.1002/elan.201200597.
26. Sinkala E, McCutcheon JE, Schuck MJ, Schmidt E, Roitman MF, Eddington DT. Electrode calibration with a microfluidic flow cell for fast-scan cyclic voltammetry. Lab Chip. 2012;12:2403–8. https://doi.org/10.1039/c2lc40168a.
27. Beebe DJ, Mensing GA, Walker GM. Physics and applications of microfluidics in biology. Annu Rev Biomed Eng. 2002;4:261–86. https://doi.org/10.1146/annurev.bioeng.4.112601.125916.
28. Zhao X-M, Xia Y, Whitesides MG. Soft lithographic methods for nano-fabrication. J Mater Chem. 1997;7:1069–74. https://doi.org/10.1039/A700145B.
29. Hensley AL, Colley AR, Ross AE. Real-time detection of melatonin using fast-scan cyclic voltammetry. Anal Chem. 2018;90:8642–50. https://doi.org/10.1021/acs.analchem.8b01976.

30. Trouillon R, Lin Y, Mellander LJ, Keighron JD, Ewing AG. Evaluating the diffusion coefficient of dopamine at the cell surface during amperometric detection: disk vs ring microelectrodes. Anal Chem. 2013;85:6421–8. https://doi.org/10.1021/ac400965d.
31. Bath BD, Michael DJ, Trafton BJ, Joseph JD, Runnels PL, Wightman RM. Subsecond adsorption and desorption of dopamine at carbon-fiber microelectrodes. Anal Chem. 2000;72:5994–6002.
32. Peairs MJ, Ross AE, Venton BJ. Comparison of Nafion- and overoxidized polypyrrole-carbon nanotube electrodes for neurotransmitter detection. Anal Methods. 2011;3:2379–86. https://doi.org/10.1039/C1AY05348E.
33. Jacobs CB, Ivanov IN, Nguyen MD, Zestos AG, Venton BJ. High temporal resolution measurements of dopamine with carbon nanotube yarn microelectrodes. Anal Chem. 2014;86:5721–7. https://doi.org/10.1021/ac404050t.